

# Energy-conserving Galerkin approximations for quasigeostrophic dynamics

Matthew Watwood<sup>a</sup>, Ian Grooms<sup>a,\*</sup>, Keith A. Julien<sup>a</sup>, K. Shafer Smith<sup>b</sup>

<sup>a</sup>*Department of Applied Mathematics, University of Colorado, Boulder, CO 80309*

<sup>b</sup>*Center for Atmosphere Ocean Science, Courant Institute of Mathematical Sciences, New York University, New York, NY 10012*

---

## Abstract

A method is presented for constructing energy-conserving Galerkin approximations to the full quasigeostrophic model with active surface buoyancy. The derivation generalizes the approach of Rocha *et al.* (2016) [1] to allow for general bases. Details are then presented for a specific set of bases: Legendre polynomials for potential vorticity and a recombined Legendre basis from Shen (1994) [2] for the streamfunction. The method is tested in the context of linear baroclinic instability calculations, where it is compared to the standard second-order finite-difference method. The Galerkin scheme is quite accurate even for a small number of basis functions  $\mathcal{N}$ , and growth rates converge much more quickly for the Galerkin scheme than for the finite-difference scheme. The Galerkin scheme can in some cases achieve the same accuracy as the finite difference scheme with ten times fewer degrees of freedom.

*Keywords:* Quasigeostrophic, Spectral, Galerkin, Legendre

---

## 1. Introduction

The well-known quasigeostrophic (QG) model describes the dynamics of extratropical oceanic and atmospheric circulations [3–5], characterized by the dominant roles of background stratification, leading to hydrostatic balance, and planetary rotation, resulting in geostrophic balance. In the case of a fluid bounded above and below by flat rigid surfaces, where the vertical velocity must vanish, the dynamics are governed by the evolution of three quantities: the quasigeostrophic potential vorticity (PV)  $q(x, y, z, t)$  and the buoyancy at the top and bottom surfaces ( $b^+(x, y, t)$  and  $b^-(x, y, t)$ , respectively). The three quantities  $q$  and  $b^\pm$  evolve according to

$$\partial_t b^+ + \mathbf{u}^+ \cdot \nabla b^+ = 0 \quad (1a)$$

$$\partial_t q + \mathbf{u} \cdot \nabla q + \beta v = 0 \quad (1b)$$

$$\partial_t b^- + \mathbf{u}^- \cdot \nabla b^- = 0. \quad (1c)$$

The equations are set in a linear tangent plane to the sphere at latitude  $\theta$ . The parameter  $\beta$  is  $(f/R) \cos(\theta)$  where  $R$  is the radius of the Earth and  $f$  is twice the rotation rate of the Earth. Hereafter the symbol  $\nabla$  is to be understood as horizontal only. The velocity is also horizontal,  $\mathbf{u} \cdot \nabla = u \partial_x + v \partial_y$ , and the velocity is incompressible  $\nabla \cdot \mathbf{u} = 0$ . The velocity is obtained from the PV and surface buoyancies by solving the following elliptic equation for the streamfunction  $\psi$

$$f_0 \partial_z \psi = b^+ \text{ at } z = H \quad (2a)$$

---

\*Corresponding author

Email address: [ian.grooms@colorado.edu](mailto:ian.grooms@colorado.edu) (Ian Grooms)

$$\nabla^2 \psi + \partial_z (S(z) \partial_z \psi) = q \quad (2b)$$

$$f_0 \partial_z \psi = b^- \text{ at } z = 0 \quad (2c)$$

and then setting  $u = -\partial_y \psi$ ,  $v = \partial_x \psi$ . The streamfunction  $\psi$  can either be set to 0 on the side boundaries, or they can be periodic. For periodic boundaries an auxiliary condition  $\int \psi = 0$  is required on the elliptic inversion. The function  $S(z)$  is  $f_0^2/N^2(z)$  where  $f_0$  is the local Coriolis parameter  $f_0 = f \sin(\theta)$  and  $N(z) > 0$  is the Brunt-Väisälä frequency, also known as the buoyancy frequency.

There are two common simplifications of this system that set either  $q$  and  $\beta$  or  $b^\pm$  to zero. Both of these simplifications are exact solutions of the full equations. Setting  $b^\pm = 0$  leads to considerable simplifications in the analysis of the system and in the development of numerical methods. For example, solutions of the system with  $b^\pm = 0$  are known to be regular and to be a regular asymptotic limit of the Navier-Stokes equations [6], and standard finite-difference approximations are known to be convergent [7].

The other simplification sets  $q = \beta = 0$ . The surface-QG model (sQG) is obtained by further setting  $b^+ = 0$  and replacing the boundary condition  $\partial_z \psi = 0$  at  $z = H$  with the condition  $\partial_z \psi \rightarrow 0$  as  $z \rightarrow \infty$ . Rigorous mathematical analysis of the inviscid sQG model is considerably more difficult than the model with  $b^\pm = 0$ . A connection of the sQG model to the three-dimensional Euler equations was made in [8], and the study of well-posedness of the sQG model is ongoing (e.g. [9]; for related results in a model with dissipation see [10, 11]). As a result of this connection between the full unsimplified QG model and the sQG model global regularity of the full QG system remains an open problem, though strong solutions are known to exist and be unique for a finite time horizon [12].

Surface buoyancy has a significant impact on the dynamics of the upper ocean [13] and on the atmosphere near the tropopause [14], and the simplified system with  $b^\pm = 0$  is unable to model these dynamics. Surface-QG is able to model the impact of surface buoyancy on atmospheric and oceanic dynamics, but its accuracy is limited by the requirement that  $\beta = 0$  which restricts validity to high latitudes and small scales. In addition, several studies have used sQG theory to infer ocean subsurface velocities using only surface buoyancy but these studies have found that the assumption  $q = 0$  prevents accurate reconstruction except near the ocean surface [15–17]. To model the interplay of surface and interior dynamics one needs the full unsimplified QG model.

The primary difficulty in constructing discretizations of the full QG model is the discretization of the vertical coordinate  $z$ . The equations do not have a particularly unusual form and any one of a variety of classical methods could be used, but particular attention is paid in the community to whether a discretization is energy-conserving. This is because simulations are often used to study the energetics of the system, e.g. the transfer of energy between horizontal and vertical scales [18–20], using integrations over long time scales. The classical second order finite difference discretization found in [4, 5, 7] conserves energy and is the standard method for simulations of the full system [18, 19, 21–23]. Higher-order alternatives are therefore desirable for the purpose of achieving equal accuracy with less cost, or higher accuracy at equal cost.

The main alternative to second order finite differences is a Galerkin approach based on [24]. The operator  $\partial_z(S(z)\partial_z \cdot)$  with homogeneous Neumann boundary conditions admits a set of eigenfunctions called ‘baroclinic modes’ that form an orthogonal basis for  $L^2(0, 1)$ . A finite number of these modes can be used as a basis for an energy-conserving Galerkin approximation of the QG equations, but the straightforward application clearly assumes that  $b^\pm = 0$  since that is the boundary condition satisfied by the basis functions. It was recently shown in [1] how the same basis could be used in a way that does not require  $b^\pm = 0$ , and that still conserves energy. Unfortunately these basis functions are not practically useful except in the case where  $S(z)$  is a constant, in which case the modes are just Fourier modes. (Precisely this Fourier baroclinic mode basis was recently used in [25], but for the simplified QG model with  $b^\pm = 0$ .)

It was proposed in [14] to simply augment the baroclinic mode basis with auxiliary functions that enable satisfaction of the inhomogeneous Neumann conditions, but this method does not conserve energy [1, 14]. An alternative orthogonal basis was developed in [26]. This basis enables both satisfaction of the inhomogeneous Neumann boundary conditions and conservation of energy in a Galerkin approximation, but the basis does not enable separation of variables in the solution of the elliptic equation and is more useful for

analysis of observational data than for high-resolution simulations of the nonlinear dynamics.

This article presents an energy-conserving Galerkin approximation scheme for the full QG system that generalizes the approach in [1] so that it can be used with any appropriate basis while allowing active surface buoyancy. We immediately specialize to a global polynomial basis based on Legendre polynomials. Legendre polynomials are a convenient basis because energy conservation uses an unweighted  $L^2$  norm. The paper is organized as follows. Our main result on the construction of an energy-conserving Galerkin approximation is found in section 2. Implementation details and a specific choice of polynomial basis are presented in section 3. The method is tested and compared to the standard finite difference method in the context of linear baroclinic instability calculations in section 4. Results are discussed and conclusions are offered in section 5.

## 2. Energy-Conserving Galerkin Approximations

The QG equations conserve energy in the form

$$E = \frac{1}{2} \int |\nabla \psi|^2 + S(z)(\partial_z \psi)^2$$

where the integral is over the volume. The first term corresponds to kinetic energy and the second to available potential energy. The proof of energy conservation is straightforward: Equation (1b) is multiplied by  $-\psi$ , followed by integration over the volume. Careful use of integration by parts together with eq. (2) and the surface buoyancy equations eq. (1a) and eq. (1c) yield the desired result. The boundary conditions at the side boundaries can be assumed to be either impenetrable or periodic.

Suppose that  $q$  will be represented as a linear combination of basis functions  $p_n^q(z)$

$$q_{\mathcal{N}} = \sum_{n=1}^{\mathcal{N}} \check{q}_n(x, y, t) p_n^q(z).$$

The notation  $\mathcal{N}$  serves to distinguish the number of basis functions  $\mathcal{N}$  from the Brunt-Väisälä frequency  $N$ . The notation for the coefficients  $\check{q}_n$  follows [1]. Similarly, suppose that  $\psi$  will be represented as a linear combination of basis functions  $p_n^\psi(z)$ , which can be different from the basis used for  $q$ :

$$\psi_{\mathcal{N}} = \sum_{n=1}^{\mathcal{N}} \check{\psi}_n(x, y, t) p_n^\psi(z).$$

There are now two approximation problems. The first is related to PV inversion: given  $q_{\mathcal{N}}$  and  $b^\pm$ , how does one obtain coefficients  $\check{\psi}_n$  for  $\psi_{\mathcal{N}}$ ? The second is related to PV evolution: given  $q_{\mathcal{N}}$  and  $\psi_{\mathcal{N}}$ , how does one obtain the tendencies  $\partial_t \check{q}_n$ ? The way that these questions are answered determines the kind of approximation being made, as well as whether the scheme conserves energy.

However these questions are answered one can always define residuals  $r_q$  and  $r_t$  related to the two approximations, along with residuals  $r_b^\pm$  related to the boundary conditions

$$r_q = q_{\mathcal{N}} - \nabla^2 \psi_{\mathcal{N}} - \partial_z (S(z) \partial_z \psi_{\mathcal{N}}) \quad (3a)$$

$$r_t = \partial_t q_{\mathcal{N}} + \mathbf{u}_{\mathcal{N}} \cdot \nabla q_{\mathcal{N}} + \beta v_{\mathcal{N}} \quad (3b)$$

$$r_b^\pm = b^\pm - \partial_z \psi_{\mathcal{N}}^\pm. \quad (3c)$$

If the boundary conditions on the PV inversion are exactly satisfied then  $r_b^\pm = 0$ . A Galerkin approximation to the PV inversion would choose the coefficients  $\check{\psi}_n$  according to the condition that the residual  $r_q$  be orthogonal to the span of the basis functions  $p_n^\psi$ .

An energy-conserving discretization should conserve energy in the following form

$$E_{\mathcal{N}} = \frac{1}{2} \int |\nabla \psi_{\mathcal{N}}|^2 + S(z)(\partial_z \psi_{\mathcal{N}})^2.$$

One can obtain an exact evolution equation for  $E_{\mathcal{N}}$  by, for example, multiplying eq. (3b) by  $-\psi_{\mathcal{N}}$  and integrating over the volume. One eliminates  $q_{\mathcal{N}}$  using eq. (3a), and then performs integrations by parts using boundary conditions eq. (3c). The result is

$$\frac{dE_{\mathcal{N}}}{dt} = - \int_x [S(z)\psi_{\mathcal{N}}\partial_t r_b]_+^+ + \int \psi_{\mathcal{N}}(\partial_t r_q - r_t). \quad (4)$$

The first integral on the right hand side of this equation is taken over the two-dimensional upper and lower surfaces; this has been indicated by the subscript  $x$  on the integral:  $\int_x$ .

Energy conservation can evidently be achieved quite simply as follows. First apply the usual Galerkin condition to the PV inversion by requiring  $r_q$  to be  $L^2$ -orthogonal to the basis functions  $p_n^\psi(z)$ ; this eliminates the term  $\int \psi_{\mathcal{N}}\partial_t r_q$  in eq. (4). Next, satisfy the boundary conditions exactly so that  $r_b^\pm = 0$ , eliminating the first term on the right hand side of eq. (4). Finally, apply a Petrov-Galerkin condition to determine the evolution  $\partial_t q_{\mathcal{N}}$  by requiring  $r_t$  to be  $L^2$ -orthogonal to the span of  $p_n^\psi$ , eliminating the last term on the right hand side of eq. (4). (This latter is a Petrov-Galerkin condition because the residual is made orthogonal to a different subspace than the one in which the approximation is sought. If  $p_n^q = p_n^\psi$  then this is just another Galerkin condition.)

The problem is that there are only  $2\mathcal{N}$  degrees of freedom — one each for  $\check{\psi}_n$  and  $\check{q}_n$  — while the above recipe yields  $2\mathcal{N} + 2$  conditions. This difficulty was avoided in [1] by making use of a clever reformulation of the PV inversion proposed by Bretherton [27]. The solution to the PV inversion eq. (2) is the same as the solution to the following reformulated problem

$$\partial_z \psi = 0 \text{ at } z = H \quad (5a)$$

$$\nabla^2 \psi + \partial_z (S(z)\partial_z \psi) = q - \frac{f_0}{N^2(z)} b^+ \delta(z - H) + \frac{f_0}{N^2(z)} b^- \delta(z) \quad (5b)$$

$$\partial_z \psi = 0 \text{ at } z = 0. \quad (5c)$$

The equivalence of these two formulations can be obtained through the Green's function formulation of the solution. There is a new residual associated with this reformulation of the inversion, defined to be

$$r_q^B = q_{\mathcal{N}} - \frac{f_0}{N^2(z)} b^+ \delta(z - H) + \frac{f_0}{N^2(z)} b^- \delta(z) - \nabla^2 \psi_{\mathcal{N}} - \partial_z (S(z)\partial_z \psi_{\mathcal{N}}). \quad (6)$$

The superscript  $B$  in  $r_q^B$  stands for ‘Bretherton.’ Using this reformulated problem to derive an evolution equation for the discretized energy yields a deceptively similar equation:

$$\frac{dE_{\mathcal{N}}}{dt} = - \int_x [S(z)\psi_{\mathcal{N}}\partial_t r_b]_+^+ + \int \psi_{\mathcal{N}}(\partial_t r_q^B - r_t). \quad (7)$$

Further simplifications are possible though, since the basis functions can now be assumed to satisfy homogeneous Neumann boundary conditions  $\partial_z p_n^\psi = 0$ , consistent with the boundary conditions of the reformulated PV inversion. These boundary conditions imply that

$$r_b^\pm = b^\pm \quad \Rightarrow \quad \partial_t r_b^\pm = -\mathbf{u}_{\mathcal{N}}^\pm \cdot \nabla b^\pm. \quad (8)$$

This implies that the first term on the right hand side of the energy budget eq. (7) is zero since  $\int_x \psi_{\mathcal{N}} \mathbf{u}_{\mathcal{N}} \cdot \nabla b = 0$ . As a consequence the energy budget takes the form

$$\frac{dE_{\mathcal{N}}}{dt} = \int \psi_{\mathcal{N}}(\partial_t r_q^B - r_t). \quad (9)$$

Energy conservation can now be achieved through the use of a Galerkin condition on the reformulated PV inversion ( $r_q^B$   $L^2$ -orthogonal to  $p_n^\psi$ ), and a Petrov-Galerkin condition on the evolution tendency ( $r_t$   $L^2$ -orthogonal to  $p_n^\psi$ ). This is essentially a re-derivation of the result in [1] using an arbitrary basis instead of the baroclinic mode basis. This derivation enables the use of practical algorithms based on finite element bases, spline bases, or polynomial bases in cases where the baroclinic mode basis of [1] is unavailable or unwieldy.

We note as a brief aside that the Galerkin condition on the PV inversion is equivalent to choosing  $\psi_{\mathcal{N}}$  to minimize a semi-norm of the error. To wit, let  $\psi_*$  be the true solution to the reformulated PV inversion with  $q = q_{\mathcal{N}}$ ; then the  $\psi_{\mathcal{N}}$  that minimizes the following semi-norm of the error

$$\|\psi_* - \psi_{\mathcal{N}}\|_q^2 = \int |\nabla(\psi_* - \psi_{\mathcal{N}})|^2 + S(z) (\partial_z(\psi_* - \psi_{\mathcal{N}}))^2 \quad (10)$$

is the same as the  $\psi_{\mathcal{N}}$  that sets the residual  $r_q^B$   $L^2$ -orthogonal to the span of the basis functions  $p_n^\psi$ . This was not precisely clear in [1] where the discussion could be misconstrued to suggest that the Galerkin condition is equivalent to minimizing the  $L^2$  norm of the error.

### 3. A Legendre basis

This section begins with general considerations associated with implementation using an arbitrary basis, and continues to consideration of a specific basis using Legendre polynomials. There are two problems to deal with: (i) computing  $\psi_{\mathcal{N}}$  from  $q_{\mathcal{N}}$  and  $b^\pm$ , and (ii) computing  $\partial_t q_{\mathcal{N}}$ .

First consider the implementation of the Galerkin condition on the reformulated PV inversion eq. (5). Assume that the basis  $p_n^\psi(z)$  satisfies homogeneous Neumann conditions. The condition that the residual in eq. (6) be  $L^2$ -orthogonal to the basis functions  $p_n^\psi$  leads to an  $\mathcal{N} \times \mathcal{N}$  linear system of the following form

$$\nabla^2 \mathbf{M} \psi - \mathbf{L} \psi = \mathbf{B} \mathbf{q} - \frac{f_0}{N^2(H)} b^+ \mathbf{p}^+ + \frac{f_0}{N^2(0)} b^- \mathbf{p}^- \quad (11)$$

where the vectors  $\psi$  and  $\mathbf{q}$  contain the Galerkin coefficients  $\check{\psi}_n$  and  $\check{q}_n$ , the vectors  $\mathbf{p}^+$  and  $\mathbf{p}^-$  have elements

$$\mathbf{p}_n^+ = p_n^\psi(H) \quad \mathbf{p}_n^- = p_n^\psi(0), \quad (12)$$

and the matrices have the following elements

$$\mathbf{M}_{i,j} = \int_0^H p_i^\psi(z) p_j^\psi(z) dz, \quad (13a)$$

$$\mathbf{L}_{i,j} = \int_0^H S(z) (\partial_z p_i^\psi(z)) (\partial_z p_j^\psi(z)) dz, \quad (13b)$$

$$\mathbf{B}_{i,j} = \int_0^H p_i^\psi(z) p_j^q(z) dz. \quad (13c)$$

The discrete PV inversion system eq. (11) can be diagonalized by a change of basis. The mass matrix  $\mathbf{M}$  is symmetric positive definite and has a Cholesky factorization

$$\mathbf{M} = \mathbf{G} \mathbf{G}^T.$$

The matrix  $\mathbf{G}^{-1} \mathbf{L} \mathbf{G}^{-T}$  is symmetric positive semi-definite, and has an orthogonal eigenvalue decomposition

$$\mathbf{G}^{-1} \mathbf{L} \mathbf{G}^{-T} = \mathbf{Q} \Sigma \mathbf{Q}^T$$

where  $\mathbf{Q}$  is real orthogonal and  $\mathbf{\Sigma}$  is diagonal. With these matrix decompositions the discrete PV inversion can be diagonalized as follows

$$\nabla^2 \mathbf{M} \psi - \mathbf{L} \psi = \mathbf{G} \mathbf{Q} (\nabla^2 \mathbf{I} - \mathbf{\Sigma}) \mathbf{Q}^T \mathbf{G}^T \psi. \quad (14)$$

The PV inversion has to be solved repeatedly during a time integration of the PV equations. An efficient implementation first computes the matrices  $\mathbf{G}$ ,  $\mathbf{Q}$ , and  $\mathbf{\Sigma}$ , then uses the diagonalization above to split the PV inversion into a set of independent two-dimensional elliptic inversions. Once the matrix factorizations have been computed, the cost to invert the PV is  $\mathcal{O}(\mathcal{N}^2)$  (plus  $\mathcal{N}$  times the cost of each two-dimensional elliptic inversion).

Each column of the matrix  $\mathbf{G}^{-T} \mathbf{Q}$  contains coefficients of a function in the basis  $p_n^\psi$ . These functions together form a basis that diagonalizes the discrete PV inversion operator. These basis functions that diagonalize the discrete PV operator are approximations to the baroclinic modes of [1] that diagonalize the continuous PV operator.

Next consider the problem of computing  $\partial_t q_{\mathcal{N}}$  via the Petrov-Galerkin condition that  $r_t$  in eq. (3b) be  $L^2$ -orthogonal to the  $p_n^\psi$  basis. This condition yields a system of the form

$$\mathbf{B} (\partial_t \mathbf{q}) = \dot{\mathbf{q}} \quad (15)$$

where the elements of the right hand side are

$$(\dot{\mathbf{q}})_n = - \int_0^H p_n^\psi (\mathbf{u}_{\mathcal{N}} \cdot \nabla q_{\mathcal{N}} + \beta v_{\mathcal{N}}) dz. \quad (16)$$

Fortunately, for basis functions consisting of polynomials or piecewise polynomials these integrals can be computed exactly, either analytically or via appropriate quadratures. Since this system needs to be solved repeatedly during a time integration, an LU decomposition of the matrix  $\mathbf{B}$  can be computed once before starting the integration.

### 3.1. A Legendre basis

The foregoing analysis applies to any set of basis functions  $p_n^q$  and  $p_n^\psi$  with the assumption  $\partial_z p_n^\psi = 0$  at the boundaries. This section considers a specific choice of the two basis sets. First, since orthogonality is of necessity defined using the  $L^2$  inner product, it is convenient to let  $p_n^q(z) = L_{n-1}(z)$  where  $L_k(z)$  is the  $k^{\text{th}}$  order Legendre polynomial, rescaled to the interval  $z \in [0, H]$ .

Legendre polynomials do not satisfy  $\partial_z L_k(z) = 0$  at the boundaries, and therefore cannot be used for  $p_n^\psi$ . Shen [2] constructs the following functions

$$\phi_k(z) = L_k(z) - \frac{k(k+1)}{(k+2)(k+3)} L_{k+2}(z). \quad (17)$$

These functions form a basis for polynomials with homogeneous Neumann conditions, and we set  $p_n^\psi(z) = \phi_{k-1}(z)$ .

With this choice of  $p_n^q$  and  $p_n^\psi$  the  $\mathbf{B}$  matrix is upper triangular with upper bandwidth 2. The mass matrix  $\mathbf{M}$  is pentadiagonal and is reasonably well-conditioned out to  $\mathcal{N} \sim 1000$ , which is larger than would be used in most applications. In fact, an even-odd permutation converts the  $\mathbf{M}$  matrix to a block-diagonal matrix with tridiagonal blocks. The elements of the matrices  $\mathbf{M}$  and  $\mathbf{B}$  are known analytically.

The structure of the  $\mathbf{L}$  matrix depends on the stratification  $S(z)$  and is in general dense. (For a finite element basis the  $\mathbf{L}$  matrix would be sparse.) The elements of  $\mathbf{L}$  can in general be computed using quadrature. In the computations described in section 4 the elements of  $\mathbf{L}$  are computed using Gauss-Legendre quadrature.

With  $\mathcal{N}$  Legendre basis functions  $q_{\mathcal{N}}$  is a polynomial in  $z$  of degree  $\leq \mathcal{N} - 1$ , while  $\psi_{\mathcal{N}}$  (and hence  $\mathbf{u}_{\mathcal{N}}$ ) is a polynomial in  $z$  of degree  $\leq \mathcal{N} + 1$ . The elements of the vector  $\dot{\mathbf{q}}$  are therefore integrals of polynomials of degree at most  $3\mathcal{N} + 1$ . These can be evaluated exactly (up to roundoff error) using Gauss-Legendre quadrature with  $1.5\mathcal{N} + 1$  nodes.

#### 4. Linear Baroclinic Instability

This section makes a preliminary assessment of the accuracy of the energy-conserving Legendre Galerkin scheme described in the preceding section by applying it to the linear quasigeostrophic baroclinic instability problem. Any configuration of the form

$$\bar{\psi} = -y\bar{u}(z), \quad \bar{q}(z) = -y \frac{d}{dz} \left( S(z) \frac{d\bar{u}}{dz} \right), \quad \bar{b}^+ = -yf_0 \frac{d\bar{u}}{dz} \Big|_{z=H}, \quad \bar{b}^- = -yf_0 \frac{d\bar{u}}{dz} \Big|_{z=0}$$

is an exact solution of the fully nonlinear QG equations eq. (1). The linearization of the QG equations about an equilibrium of this form is

$$\partial_t b^+ + \bar{u}^+ \partial_x b^+ - \left( f_0 \frac{d\bar{u}}{dz} \right)_{z=H} v^+ = 0 \quad (18a)$$

$$\partial_t q + \bar{u} \partial_x q + (\partial_y \bar{q} + \beta) v = 0 \quad (18b)$$

$$\partial_t b^- + \bar{u}^- \partial_x b^- - \left( f_0 \frac{d\bar{u}}{dz} \right)_{z=0} v^- = 0. \quad (18c)$$

Linear instability about an equilibrium of this form is called ‘baroclinic instability.’ The linear equations vary only in  $z$ , so it is convenient to Fourier transform in the horizontal direction, and to assume exponential growth in time with the form  $e^{-ik_x ct}$  where  $k_x$  is the wavenumber in the  $x$  direction and  $c$  is the wave phase speed. Also replacing  $f_0 d\bar{u}/dz$  by  $-\partial_y \bar{b}$  on the boundaries leads to equations of the form

$$\bar{u}^+ \hat{b}^+ + (\partial_y \bar{b}^+) \hat{\psi}^+ = c \hat{b}^+ \quad (19a)$$

$$\bar{u} \hat{q} + (\partial_y \bar{q} + \beta) \hat{\psi} = c \hat{q} \quad (19b)$$

$$\bar{u}^- \hat{b}^- + (\partial_y \bar{b}^-) \hat{\psi}^- = c \hat{b}^- \quad (19c)$$

where  $\hat{q}$  is the Fourier transform of  $q$  and  $\hat{b}^\pm$  is the Fourier transform of  $b^\pm$ . The standard energy-conserving second-order finite difference discretization of the linear stability problem is described in Appendix B.

##### 4.1. Galerkin Discrete Linear Baroclinic Instability

To discretize this system according to the methods described in the previous section, one makes Galerkin approximations to both the equilibrium state and the perturbations, then one imposes Galerkin and Petrov-Galerkin conditions on the residuals. First consider how to construct the appropriate Galerkin approximation to the equilibrium state. Although the equilibrium can be completely described by  $\bar{u}(z)$ , the correct approach within the method described in the foregoing section is to first produce a Galerkin approximation to  $\partial_y \bar{q}$  and then invert to find  $\bar{u}$ . The expansion coefficients in the approximation of  $\partial_y \bar{q}$  are arranged into the vector  $\bar{\mathbf{q}}_y$ , whose entries are

$$(\bar{\mathbf{q}}_y)_n = \frac{\int_0^H p_n^q(z) (\partial_y \bar{q}) dz}{\int_0^H (p_n^q(z))^2 dz}.$$

(This expression assumes that the basis functions  $p_n^q(z)$  are  $L^2$ -orthogonal, which is true for the Legendre basis considered here. For a non-orthogonal basis one would have to solve a linear system to find  $\bar{\mathbf{q}}_y$ .) Once this vector is available, the coefficients in the Galerkin approximation of  $\bar{u}$  are obtained by solving the following system

$$\mathbf{L} \bar{\mathbf{u}} = -\mathbf{B} \bar{\mathbf{q}}_y + \frac{f_0}{N^2(H)} (\partial_y \bar{b}^+) \mathbf{p}^+ - \frac{f_0}{N^2(0)} (\partial_y \bar{b}^-) \mathbf{p}^-. \quad (20)$$

The vectors  $\mathbf{p}^\pm$  are defined in eq. (12).

Unfortunately the matrix  $\mathbf{L}$  is singular: its first row and column are zero because  $p_1^\psi(z) = 1$  and  $\partial_z p_1^\psi = 0$ . Fortunately the right hand side is always compatible: the first entry of the right hand side is always zero as well. This statement is substantiated in Appendix A. The first entry of  $\bar{\mathbf{u}}$  is not constrained by the linear system above; it corresponds to the depth-independent component of  $\bar{u}(z)$ . The first Galerkin coefficient of  $\bar{u}$  can simply be set to

$$\bar{\mathbf{u}}_1 = \frac{\int_0^H p_1^\psi(z) \bar{u} dz}{\int_0^H (p_1^\psi(z))^2 dz}.$$

The remaining entries of  $\bar{\mathbf{u}}$  are obtained by solving the lower-right  $\mathcal{N} - 1 \times \mathcal{N} - 1$  block of eq. (20).

Next consider how to construct an appropriate Galerkin approximation to the perturbations about the equilibrium. The Galerkin approximations to the perturbations  $\hat{q}$  and  $\hat{\psi}$  will have coefficients stored in the vectors  $\mathbf{q}$  and  $\boldsymbol{\psi}$ , respectively. These coefficients are related through the Fourier transform of eq. (11), which is

$$-(k_x^2 + k_y^2) \mathbf{M} \boldsymbol{\psi} - \mathbf{L} \boldsymbol{\psi} = \mathbf{B} \mathbf{q} - \frac{f_0}{N^2(H)} b^+ \mathbf{p}^+ + \frac{f_0}{N^2(0)} b^- \mathbf{p}^-. \quad (21)$$

With Galerkin approximations to the equilibrium and perturbations in hand, one next inserts these approximations into eq. (19b) and requires the residual to be orthogonal to  $p_n^\psi$ . One also inserts  $\bar{u}_{\mathcal{N}}$  in place of  $\bar{u}$  in eq. (19a) and eq. (19c), yielding the following linear system

$$\bar{u}_{\mathcal{N}}^+ \hat{b}^+ + (\partial_y \bar{b}^+) \hat{\psi}_{\mathcal{N}}^+ = c \hat{b}^+ \quad (22a)$$

$$\bar{\mathbf{U}} \mathbf{q} + (\bar{\mathbf{Q}}_y + \beta \mathbf{M}) \boldsymbol{\psi} = c \mathbf{B} \mathbf{q} \quad (22b)$$

$$\bar{u}_{\mathcal{N}}^- \hat{b}^- + (\partial_y \bar{b}^-) \hat{\psi}_{\mathcal{N}}^- = c \hat{b}^-. \quad (22c)$$

Note that  $\hat{\psi}_{\mathcal{N}}^\pm = \boldsymbol{\psi} \cdot \mathbf{p}^\pm$ , where the vectors  $\mathbf{p}^\pm$  are defined in eq. (12). With this notation the linear system eq. (22) can be written

$$\bar{u}_{\mathcal{N}}^+ \hat{b}^+ + (\partial_y \bar{b}^+) \mathbf{p}^+ \cdot \boldsymbol{\psi} = c \hat{b}^+ \quad (23a)$$

$$\bar{\mathbf{U}} \mathbf{q} + (\bar{\mathbf{Q}}_y + \beta \mathbf{M}) \boldsymbol{\psi} = c \mathbf{B} \mathbf{q} \quad (23b)$$

$$\bar{u}_{\mathcal{N}}^- \hat{b}^- + (\partial_y \bar{b}^-) \mathbf{p}^- \cdot \boldsymbol{\psi} = c \hat{b}^-. \quad (23c)$$

The matrices  $\bar{\mathbf{U}}$  and  $\bar{\mathbf{Q}}_y$  have the following entries

$$\bar{\mathbf{U}}_{ij} = \int_0^H p_i^\psi(z) p_j^q(z) \bar{u}_{\mathcal{N}}(z) dz \quad (24)$$

$$(\bar{\mathbf{Q}}_y)_{ij} = \int_0^H p_i^\psi(z) p_j^\psi(z) (\partial_y \bar{q}_{\mathcal{N}}(z)) dz. \quad (25)$$

To obtain an eigenvalue problem, the vector  $\boldsymbol{\psi}$  can be eliminated using eq. (21)

$$\boldsymbol{\psi} = -((k_x^2 + k_y^2) \mathbf{M} + \mathbf{L})^{-1} \mathbf{B} \mathbf{q} + \frac{f_0}{N^2(H)} b^+ \mathbf{p}^+ - \frac{f_0}{N^2(0)} b^- \mathbf{p}^-. \quad (26)$$



For notational convenience the following vectors have been defined

$$\boldsymbol{\psi}^\pm = ((k_x^2 + k_y^2)\mathbf{M} + \mathbf{L})^{-1} \mathbf{p}^\pm. \quad (27)$$

The matrix  $(k_x^2 + k_y^2)\mathbf{M} + \mathbf{L}$  is invertible as long as  $k_x^2 + k_y^2 \neq 0$  since  $\mathbf{M}$  is positive definite and  $\mathbf{L}$  is positive semi-definite.

Eliminating  $\boldsymbol{\psi}$  leads to a generalized eigenvalue problem of the form

$$\left[ \begin{array}{c|c|c} a_{11} & \mathbf{a}_{12}^T & a_{13} \\ \hline \mathbf{a}_{21} & \mathbf{A}_{22} & \mathbf{a}_{23} \\ \hline a_{31} & \mathbf{a}_{32}^T & a_{33} \end{array} \right] \begin{pmatrix} \hat{b}^+ \\ \mathbf{q} \\ \hat{b}^- \end{pmatrix} = c \left[ \begin{array}{c|c|c} 1 & \mathbf{0}^T & 0 \\ \hline \mathbf{0} & \mathbf{B} & \mathbf{0} \\ \hline 0 & \mathbf{0}^T & 0 \end{array} \right] \begin{pmatrix} \hat{b}^+ \\ \mathbf{q} \\ \hat{b}^- \end{pmatrix} \quad (28)$$

where the matrix on the left hand side has the following entries

$$a_{11} = \bar{u}_N^+ + \frac{f_0}{N^2(H)} (\partial_y \bar{b}^+) \mathbf{p}^+ \cdot \boldsymbol{\psi}^+ \quad (29a)$$

$$\mathbf{a}_{12} = -\frac{f_0}{N^2(H)} (\partial_y \bar{b}^+) \mathbf{B}^T ((k_x^2 + k_y^2)\mathbf{M} + \mathbf{L})^{-1} \mathbf{p}^+ \quad (29b)$$

$$a_{13} = -\frac{f_0}{N^2(H)} (\partial_y \bar{b}^+) \mathbf{p}^+ \cdot \boldsymbol{\psi}^- \quad (29c)$$

$$\mathbf{a}_{21} = (\bar{\mathbf{Q}}_y + \beta \mathbf{M}) \boldsymbol{\psi}^+ \quad (29d)$$

$$\mathbf{A}_{22} = \bar{\mathbf{U}} - (\bar{\mathbf{Q}}_y + \beta \mathbf{M}) ((k_x^2 + k_y^2)\mathbf{M} + \mathbf{L})^{-1} \mathbf{B} \quad (29e)$$

$$\mathbf{a}_{23} = -(\bar{\mathbf{Q}}_y + \beta \mathbf{M}) \boldsymbol{\psi}^- \quad (29f)$$

$$a_{31} = \frac{f_0}{N^2(0)} (\partial_y \bar{b}^-) \mathbf{p}^- \cdot \boldsymbol{\psi}^+ \quad (29g)$$

$$\mathbf{a}_{32} = -\frac{f_0}{N^2(0)} (\partial_y \bar{b}^-) \mathbf{B}^T ((k_x^2 + k_y^2)\mathbf{M} + \mathbf{L})^{-1} \mathbf{p}^- \quad (29h)$$

$$a_{33} = \bar{u}_N^- - \frac{f_0}{N^2(0)} (\partial_y \bar{b}^-) \mathbf{p}^- \cdot \boldsymbol{\psi}^-. \quad (29i)$$

To solve a specific linear baroclinic instability problem, one chooses external parameters  $f_0$ ,  $\beta$ , and  $N^2(z)$ , and an equilibrium state  $\bar{u}(z)$ . Then one computes eigenvalues of the generalized eigenvalue problem, typically over some range of values of  $k_x$  and  $k_y$ ; eigenvalues  $c$  with positive imaginary part are associated with linearly unstable solutions. Code to set up and solve the Galerkin and finite-difference linear stability problems is available in [28].

#### 4.2. The Eady Problem

The classical Eady problem is defined by constant  $N^2(z)$ , linear velocity  $\bar{u}(z)$ , and  $\beta = 0$ . In this case the baroclinic modes of [1] are simply Fourier modes and are tractable analytically and computationally. The exact linear perturbation equations eq. (19) are also analytically solvable in the Eady problem (see, e.g. [5, Chapter 6]), which makes for a good test problem. This section sets  $N^2(z) = f_0^2 = 1$ ,  $H = 1$ , and  $\bar{u} = z$ . The most unstable solutions are found along the axis  $k_y = 0$ , so the generalized eigenvalue problem is solved for a range of  $k_x$ .

Figure 1 shows the results of the linear Eady problem with  $\mathcal{N} = 7$ , compared to the analytical results from [5, Chapter 6]. The growth rates (upper left) and wave speeds (lower left) as a function of  $k_x$  are well

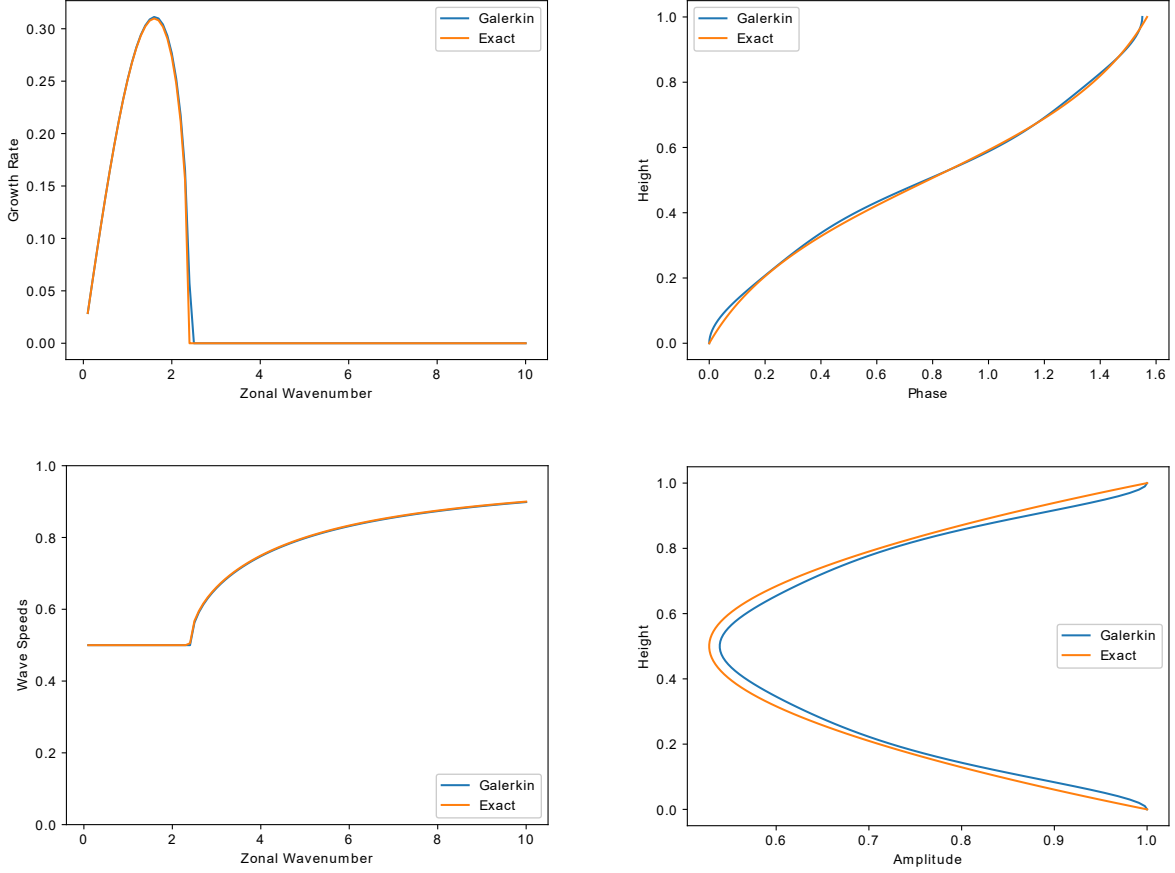


Figure 1: Comparing Galerkin with  $\mathcal{N} = 7$  (blue) to exact results (orange) in the Eady Problem with  $k_y = 0$ . Upper left: Growth rates as a function of  $k_x$ . Lower left: Wave speeds (real part of the eigenvalue  $c$ ) as a function of  $k_x$ . Upper right: Complex phase as a function of  $z$  for the eigenfunction associated with the fastest-growing mode. Lower right: Amplitude as a function of  $z$  for the eigenfunction associated with the fastest-growing mode, normalized to 1 at  $z = 0$ .

reproduced with only  $\mathcal{N} = 7$  basis functions. (Note that the streamfunction of the most unstable mode,  $k_x \approx 1.6$ , is approximated with a polynomial of degree 9.) The amplitude (upper right) and phase (lower right) of the eigenfunction corresponding to the most unstable mode are also very accurate using only  $\mathcal{N} = 7$ .

Figure 2 shows the absolute value of the error in the growth rate of the most unstable mode as a function of  $\mathcal{N}$  for both the finite-difference discretization (see Appendix B) and the Galerkin approximation. Note that in the finite-difference approximation there are  $\mathcal{N}$  degrees of freedom, while in the Galerkin approximation there are  $\mathcal{N} + 2$  degrees of freedom: one for each Galerkin coefficient and one for each surface buoyancy. The error in the Galerkin approximation decreases as  $\mathcal{O}(\mathcal{N}^{-3})$ , while the error in the finite difference approximation decreases only quadratically. Convergence of spectral methods can be limited by lack of smoothness in the functions being approximated, but the eigenfunctions of the Eady problem are entire functions expressible as a sum of hyperbolic sine and cosine functions [5]. The fact that the Galerkin method converges algebraically rather than exponentially is therefore presumably due to the mismatch between the homogeneous boundary conditions satisfied by the basis functions  $p_n^\psi$  and the inhomogeneous boundary conditions satisfied by the true eigenfunctions.

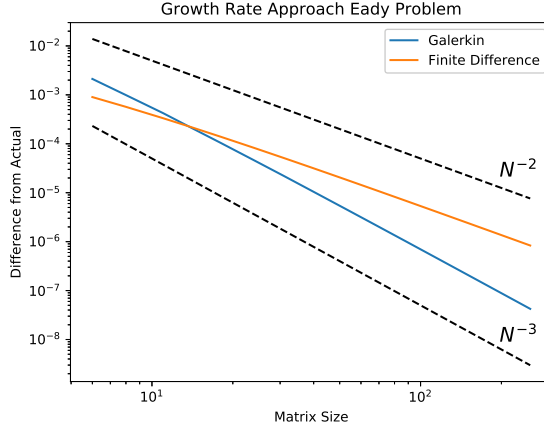


Figure 2: Error in the growth rate of the fastest growing mode as a function of  $\mathcal{N}$  for the Galerkin (blue) and finite-difference (orange) methods.

#### 4.3. The Phillips Problem

The Eady problem is a classical linear baroclinic instability problem, and the ocean-Charney problem is a more common type of instability observed in the oceans [29]. Another classical linear baroclinic instability problem that, unlike the Eady problem, is observed in the oceans occurs when the potential vorticity gradient  $d\bar{q}/dy$  changes sign in the interior of the fluid. The canonical representation of this kind of instability is present in the ‘Phillips’ problem which is distinguished by an equilibrium velocity that has zero shear at the top and bottom surface, and a single sign change in the potential vorticity in the interior. We construct a ‘Phillips’ problem of this type as follows

$$f_0 = N(z) = H = 1, \quad \beta = 3.1, \quad \bar{u} = -\pi^{-1} \cos(\pi z), \quad \bar{q} = \pi \cos(\pi z)y. \quad (30)$$

The total potential vorticity gradient is  $3.1 + \pi \cos(\pi z)$ . The negative potential vorticity gradient near the top boundary has small amplitude, and as a result the equilibrium is only slightly above the threshold for instability. There is only a small range of wavenumbers near  $k_x = 3$  that are unstable, as shown in the left panel of fig. 3.

The center and right panels of fig. 3 show the absolute value of the error in the growth rate at  $k_x = 3$  as a function of  $\mathcal{N}$  for both the Galerkin (center) and finite-difference (right) methods. The center panel uses a logarithmic scale on the growth rate axis and a linear scale on the  $\mathcal{N}$  axis to show that the Galerkin method is converging exponentially rather than algebraically, at least until it reaches the level of roundoff error near  $\mathcal{N} = 80$ . The right panel uses a logarithmic scaling on both axes to show that the finite-difference method is converging quadratically, as usual. Exponential convergence is expected for the Galerkin method in this case, since the eigenfunctions are smooth and have the same homogeneous Neumann boundary conditions as the basis functions  $p_n^\psi$ . Note that the accuracy of the finite difference scheme with  $\mathcal{N} = 256$  can be achieved by the Galerkin scheme with ten times fewer degrees of freedom.

#### 4.4. A Charney-Type Problem

The instability in the Eady problem is driven by interacting edge waves, and is therefore of a type not often seen in the atmosphere or ocean. A more common type of instability in the ocean is driven by the interaction of an edge wave with a Rossby wave in the interior of the fluid [29]. A canonical problem describing this kind of instability is the Charney problem, but the canonical Charney problem is posed in a semi-infinite domain with no upper surface. A Charney-type problem more relevant to the ocean is defined by having a nonzero shear  $d\bar{u}/dz$  at the top surface, zero shear at the bottom surface, and a constant potential vorticity gradient  $d\bar{q}/dy$  in the interior. We construct such a Charney-type problem with

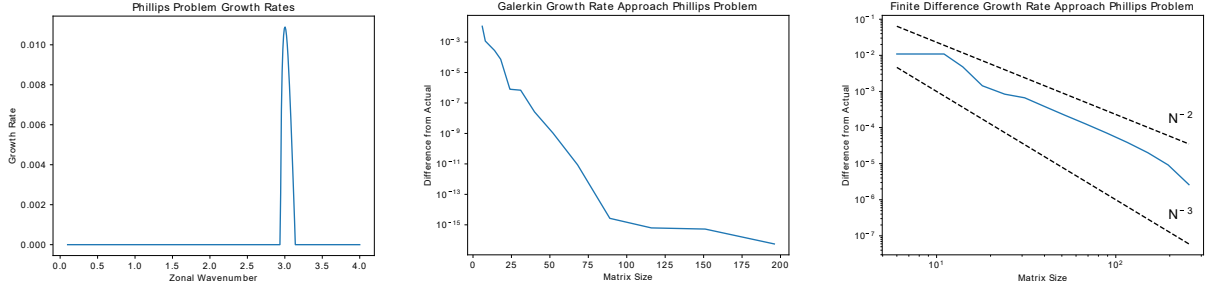


Figure 3: Growth rates in the Phillips problem. Left: Growth rates versus  $k_x$  for the Galerkin method with  $\mathcal{N} = 256$ . Center: Error in the growth rate at  $k_x = 3$  as a function of  $\mathcal{N}$  for the Galerkin method. Right: Error in the growth rate at  $k_x = 3$  as a function of  $\mathcal{N}$  for the finite-difference method.

exponential rather than constant stratification to demonstrate the ability of the Galerkin method to handle non-constant stratification. The equilibrium state is defined as follows

$$f_0 = \beta = H = 1, \quad N^2(z) = e^{6z-6}, \quad \bar{u} = \frac{1}{54} (3e^{6z-6}(6z-1) - 2 - e^{-6}), \quad \bar{q} = -2y. \quad (31)$$

Both the stratification and the velocity are surface-intensified (the velocity  $\bar{u}(z)$  is shown in the lower right panel of fig. 4), which leads to surface-intensification of the unstable linear eigenfunctions.

Figure 4 shows the results of the linear Charney-type problem. The upper left panel of fig. 4 shows the growth rate as a function of  $k_x$  for  $\mathcal{N} = 32$  and 256. The upper right panel of fig. 4 shows the absolute value of the error in the growth rate of the most unstable mode as a function of  $\mathcal{N}$  for both the finite-difference discretization and the Galerkin approximation. The growth rate in the Galerkin method converges approximately quintically ( $\mathcal{O}(\mathcal{N}^{-5})$ ) while the finite-difference method converges approximately quadratically. Unlike the Eady problem, the Galerkin approximation is more accurate than the finite difference approximation for the entire range of  $\mathcal{N}$ . The accuracy of the finite difference scheme with  $\mathcal{N} = 256$  can be achieved with the Galerkin scheme with ten times fewer degrees of freedom.

A distinctive feature of the Charney-type problem is the presence of weak instability at small scales (large  $k_x$ ), as shown in the upper left panel of fig. 4. Representation of the small-scale instabilities clearly requires large  $\mathcal{N}$ ; this is true in both the Galerkin and finite-difference methods, which behave similarly at small scales (not shown). These small-scale unstable modes result from the interaction of a Rossby wave in a thin layer near the upper surface with an edge wave propagating along the surface. The lower-right panel of fig. 4 shows the eigenfunction structure  $|\hat{q}_{\mathcal{N}}(z)|$  at both  $k_x = 5$  and  $k_x = 8$ , both computed using  $\mathcal{N} = 256$ ; the near-surface layer is evident in the eigenfunction at  $k_x = 8$ . (See also fig. 7 of [1].) Even at  $\mathcal{N} = 256$  these modes are clearly poorly resolved. As a result of the near-surface nature of the instability, the instability is especially sensitive to the representation of the equilibrium background velocity  $\bar{u}(z)$  near the boundary. The lower left panel of fig. 4 shows the background velocity  $\bar{u}$  along with the Galerkin approximations  $\bar{u}_{\mathcal{N}}(z)$  for  $\mathcal{N} = 4, 8, 16$ , and 32. Convergence of  $\bar{u}_{\mathcal{N}}(z)$  to  $\bar{u}(z)$  is slow near the upper boundary because the basis functions satisfy  $\partial_z p_n^\psi = 0$  at the boundary, while the equilibrium background profile  $\bar{u}(z)$  has  $\partial_z \bar{u} \neq 0$  at the boundary. This slow convergence of  $\bar{u}_{\mathcal{N}}(z)$  near the boundary is ultimately why the small-scale (high  $k_x$ ) instability shown in the upper panel of fig. 4 converges slowly.

## 5. Conclusions

This article presents an energy-conserving Galerkin approximation scheme for the full QG system with nonzero surface buoyancy. The scheme generalizes the Galerkin scheme of [1]. The method in [1] uses Sturm-Liouville eigenfunctions as a basis to approximate both the potential vorticity  $q$  and the streamfunction  $\psi$ , but these functions are in most cases computationally intractable. The scheme presented here generalizes the method of [1] to allow an arbitrary basis for  $q$  and any basis for  $\psi$  that satisfies homogeneous Neumann

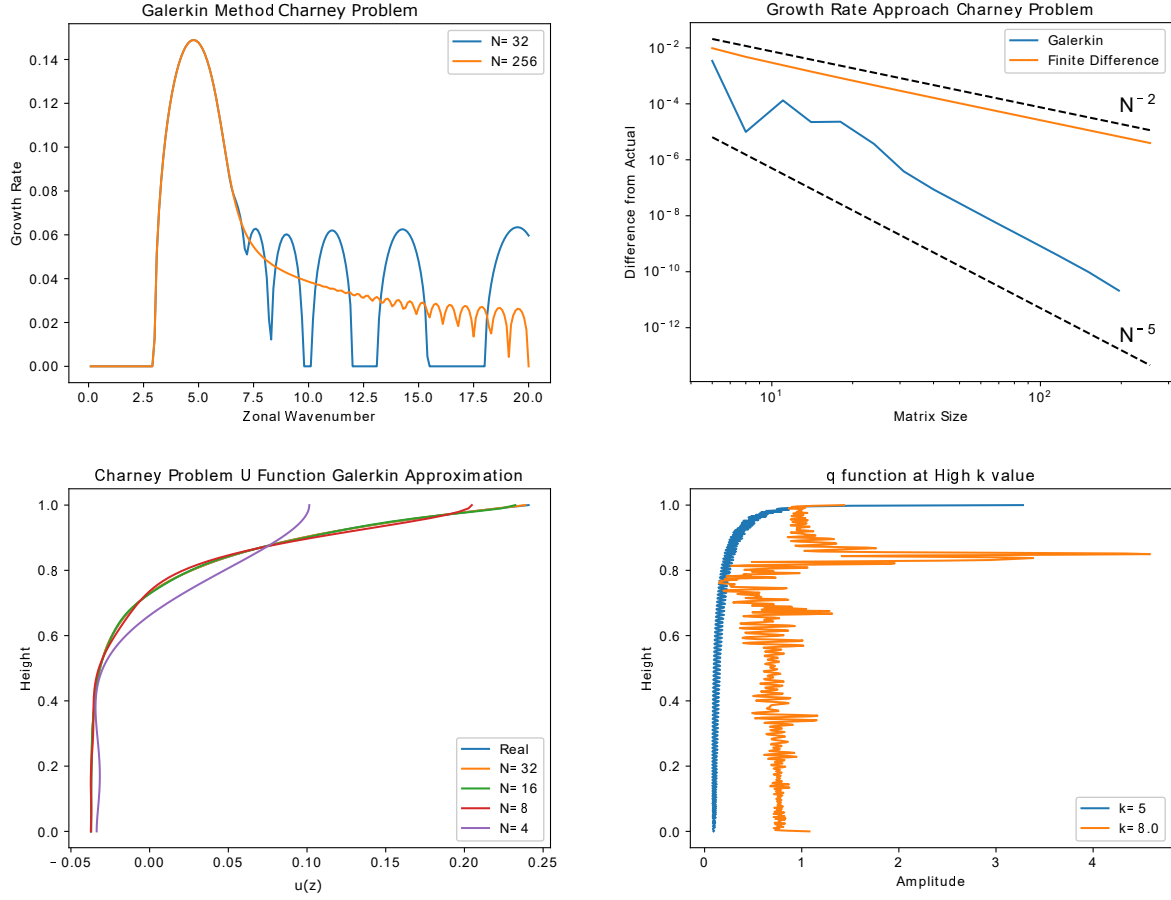


Figure 4: Growth rates in the Charney-type problem. Upper left: Growth rates versus  $k_x$  for the Galerkin method with  $N = 32$  (blue) and  $N = 256$  (orange). Upper right: Error in the growth rate of the fastest-growing mode as a function of  $N$  for the Galerkin (blue) and finite-difference (orange) methods. Lower left: Background velocity  $\bar{u}(z)$  (blue) and Galerkin approximations  $\bar{u}_N(z)$  for  $N = 4, 8, 16$ , and  $32$ . Lower right: Amplitude of the eigenfunction  $|\hat{q}(z)|$  at  $k_x = 5$  (blue) and  $8$  (orange) using  $N = 256$ .

boundary conditions at the top and bottom surfaces. Attention is then focused on a Legendre basis for  $q$ , and a recombined Legendre basis from [2] for  $\psi$ . Legendre bases were used rather than Chebyshev because energy conservation requires the use of unweighted  $L^2$  inner products, and Legendre polynomials are more convenient with this inner product.

The method was tested and compared to the standard energy-conserving second-order finite-difference method in the context of linear stability calculations. In these calculations the Galerkin scheme converged much faster than the finite difference scheme. The eigenvalues computed with the finite difference scheme converged quadratically, while those computed with the Galerkin scheme converged either at fifth order (in cases with nonzero surface buoyancy) or exponentially (with zero surface buoyancy). The absolute value of the error in the growth rates was also generally much smaller in the Galerkin scheme than in the finite difference scheme. In the Charney-type and Phillips stability problems can achieve the same accuracy as the finite difference scheme with approximately ten times fewer grid points.

The scheme presented here is ultimately intended for us in a fully nonlinear setting, and the linear stability computations only give limited insight into the accuracy of the scheme for nonlinear problems. The scheme presented here will be tested in a fully nonlinear setting in future work. Finite element bases rather than a global polynomial basis could also be explored as a means of enhancing sparsity in future work.

## Appendix A. Compatibility of the system eq. (20)

The first entry of the right hand side of eq. (20) is a sum of three components, and this appendix demonstrates that the sum of these three components is zero. The proof relies on the fact that  $p_1^\psi(z) = 1$ ,  $p_j^q(z) = L_{j-1}(z)$ , and  $p_1^q(z) = 1$ .

The first component of the right hand side of eq. (20) is the first entry of the vector  $-\mathbf{B}\bar{\mathbf{q}}_y$ . The first row of the matrix  $\mathbf{B}$  has elements

$$\int_0^H p_1^\psi(z) p_j^q(z) dz = \int_0^H p_j^q(z) dz = H \delta_{1j}$$

where  $\delta_{ij}$  is the Kronecker delta. The first entry of  $-\mathbf{B}\bar{\mathbf{q}}_y$  is thus simply the first entry of  $\bar{\mathbf{q}}_y$  multiplied by  $-H$ .

The first entry of  $\bar{\mathbf{q}}_y$  is

$$\begin{aligned} \frac{\int_0^H p_1^q(z) \partial_y \bar{q}(z) dz}{\int_0^H (p_1^q(z))^2 dz} &= -\frac{1}{H} \int_0^H \frac{d}{dz} \left( S(z) \frac{d\bar{u}}{dz} \right) dz \\ &= \frac{1}{H} \left[ S(0) \frac{d\bar{u}}{dz} \Big|_{z=0} - S(H) \frac{d\bar{u}}{dz} \Big|_{z=H} \right] \\ &= \frac{1}{H} \left[ \frac{f_0}{N^2(H)} \partial_y \bar{b}^+ - \frac{f_0}{N^2(0)} \partial_y \bar{b}^- \right]. \end{aligned}$$

Multiplying this by  $-H$  results in an expression that exactly cancels the remaining two components on the right hand side of eq. (20).

## Appendix B. Finite Difference Discretization

This section recalls the standard finite-difference discretization of the QG equations, which can be found in, e.g., [4] and [5]. A derivation with careful treatment of surface buoyancy and unequal spacing can be found in [23].

Let  $\Delta_z = 1/\mathcal{N}$  be the grid spacing where  $\mathcal{N}$  is the number of vertical levels. Both  $\psi$  and  $q$  are tracked at  $\mathcal{N}$  points starting at  $z_1 = \Delta_z/2$  and ending at  $z_{\mathcal{N}} = 1 - \Delta_z/2$ . The finite difference approximation to  $\nabla^2 \psi + \partial_z(S(z)\partial_z \psi)$  at an interior point  $z_k$  ( $k \neq 1, \mathcal{N}$ ) is

$$(\nabla^2 \psi + \partial_z(S(z)\partial_z \psi))|_{z=z_k} \approx \nabla^2 \psi_k + \frac{1}{\Delta_z} \left[ S_k \frac{\psi_{k+1} - \psi_k}{\Delta_z} - S_{k-1} \frac{\psi_k - \psi_{k-1}}{\Delta_z} \right] = q_k \quad (\text{B.1})$$

where  $S_k = S(k\Delta_z)$ . At the boundaries we have the following approximations

$$(\nabla^2 \psi + \partial_z(S(z)\partial_z \psi))|_{z=z_1} \approx \nabla^2 \psi_1 + \frac{1}{\Delta_z} \left[ S_1 \frac{\psi_2 - \psi_1}{\Delta_z} - \frac{f_0}{N^2(0)} b^- \right] = q_1 \quad (\text{B.2})$$

$$(\nabla^2 \psi + \partial_z(S(z)\partial_z \psi))|_{z=z_{\mathcal{N}}} \approx \nabla^2 \psi_{\mathcal{N}} + \frac{1}{\Delta_z} \left[ \frac{f_0}{N^2(H)} b^+ - S_{\mathcal{N}-1} \frac{\psi_{\mathcal{N}} - \psi_{\mathcal{N}-1}}{\Delta_z} \right] = q_{\mathcal{N}}. \quad (\text{B.3})$$

As discussed in [23], if one defines

$$Q_1 = q_1 + \frac{f_0}{\Delta_z N^2(0)} b^- = \nabla^2 \psi_1 + \frac{1}{\Delta_z} \left[ S_1 \frac{\psi_2 - \psi_1}{\Delta_z} \right], \quad (\text{B.4a})$$

$$Q_{\mathcal{N}} = q_{\mathcal{N}} - \frac{f_0}{\Delta_z N^2(H)} b^+ = \nabla^2 \psi_{\mathcal{N}} - \frac{1}{\Delta_z} \left[ S_{\mathcal{N}-1} \frac{\psi_{\mathcal{N}} - \psi_{\mathcal{N}-1}}{\Delta_z} \right] \quad (\text{B.4b})$$

Then the fully nonlinear system dynamics are controlled entirely by the following system

$$\partial_t Q_1 + J[\psi_1, Q_1] + \beta \partial_x \psi_1 = 0 \quad (\text{B.5a})$$

$$\partial_t q_k + J[\psi_k, Q_k] + \beta \partial_x \psi_k = 0, \quad k = 2, \dots, \mathcal{N} - 1 \quad (\text{B.5b})$$

$$\partial_t Q_{\mathcal{N}} + J[\psi_{\mathcal{N}}, Q_{\mathcal{N}}] + \beta \partial_x \psi_{\mathcal{N}} = 0. \quad (\text{B.5c})$$

The only caveat is that by evolving this system one knows  $Q_1$  and  $Q_{\mathcal{N}}$  but not  $b^\pm$  or  $q_1$  and  $q_{\mathcal{N}}$ , but the dynamics of  $\psi_k$  are completely controlled by the above system: eq. (B.5) for the dynamics and eq. (B.1) and eq. (B.4) for the PV inversion.

The discrete version of the linear stability problem is straightforward in the finite difference approximation. One can start with eq. (19) and then discretize as described above. The discrete finite difference problem takes the form of the following generalized eigenvalue problem

$$[\bar{\mathbf{U}}_{FD} ((k_x^2 + k_y^2)\mathbf{I} + \mathbf{L}_{FD}) - (\bar{\mathbf{Q}}_{y,FD} + \beta\mathbf{I})] \boldsymbol{\psi} = c [(k_x^2 + k_y^2)\mathbf{I} + \mathbf{L}_{FD}] \boldsymbol{\psi}.$$

The matrix  $\bar{\mathbf{U}}_{FD}$  is diagonal with diagonal elements  $\bar{u}(z_k)$ . The matrix  $\mathbf{L}_{FD}$  is tridiagonal with the form

$$\mathbf{L}_{FD} = \frac{1}{\Delta_z^2} \begin{bmatrix} S_1 & -S_1 & 0 & \cdots & 0 \\ -S_1 & S_1 + S_2 & -S_2 & & \vdots \\ \vdots & \ddots & \ddots & \ddots & \vdots \\ & -S_{k-1} & S_{k-1} + S_k & -S_k & \\ \vdots & \ddots & \ddots & \ddots & \vdots \\ 0 & \cdots & 0 & -S_{\mathcal{N}-1} & S_{\mathcal{N}-1} \end{bmatrix}$$

The matrix  $\bar{\mathbf{Q}}_{y,FD}$  is also diagonal. If one defines a vector  $\bar{\mathbf{u}}$  whose elements are  $\bar{u}(z_k)$ , the diagonal elements of  $\bar{\mathbf{Q}}_{y,FD}$  are the elements of the vector  $\mathbf{L}_{FD}\bar{\mathbf{u}}$ . It is interesting to note that in the Galerkin method the approximate velocity profile  $\bar{u}_{\mathcal{N}}(z)$  is derived from the potential vorticity gradient and the surface buoyancy gradients, while in the finite-difference approximation the potential vorticity gradient is derived from the velocity profile.

## References

- [1] C. B. Rocha, W. R. Young, I. Grooms, On galerkin approximations of the surface active quasigeostrophic equations, *J. Phys. Ocean.* 46 (2016) 125–139.
- [2] J. Shen, Efficient spectral-Galerkin method I. Direct solvers of second-and fourth-order equations using Legendre polynomials, *SIAM J. Sci. Comput.* 15 (1994) 1489–1505.
- [3] A. Majda, *Introduction to PDEs and Waves for the Atmosphere and Ocean*, American Mathematical Society, 2003.
- [4] J. Pedlosky, *Geophysical Fluid Dynamics*, second edition ed., Springer-Verlag New York, 1987.
- [5] G. K. Vallis, *Atmospheric and oceanic fluid dynamics*, Cambridge University Press, 2017.
- [6] A. J. Bourgeois, J. T. Beale, Validity of the quasigeostrophic model for large-scale flow in the atmosphere and ocean, *SIAM J. Math. Anal.* 25 (1994) 1023–1068.
- [7] T. Colin, The Cauchy problem and the continuous limit for the multilayer model in geophysical fluid dynamics, *SIAM J. Math. Anal.* 28 (1997) 516–529.
- [8] P. Constantin, A. J. Majda, E. Tabak, Formation of strong fronts in the 2-D quasigeostrophic thermal active scalar, *Nonlinearity* 7 (1994) 1495.
- [9] P. Constantin, H. Nguyen, Global weak solutions for SQG in bounded domains, *Comm. Pure Appl. Math.* (2017).
- [10] G. Lapeyre, Surface quasi-geostrophy, *Fluids* 2 (2017) 7.
- [11] M. D. Novack, A. F. Vasseur, Global in time classical solutions to the 3D quasi-geostrophic system for large initial data, *Commun. Math. Phys.* 358 (2018) 237–267.
- [12] A. Bennett, P. Kloeden, The periodic quasigeostrophic equations: existence and uniqueness of strong solutions, *P. Roy. Soc. Edinb. A* 91 (1982) 185–203.

- [13] G. Lapeyre, P. Klein, Dynamics of the upper oceanic layers in terms of surface quasigeostrophy theory, *J. Phys. Ocean.* 36 (2006) 165–176.
- [14] R. Tulloch, K. S. Smith, Quasigeostrophic turbulence with explicit surface dynamics: Application to the atmospheric energy spectrum, *J. Atmos. Sci.* 66 (2009) 450–467.
- [15] J. LaCasce, A. Mahadevan, Estimating subsurface horizontal and vertical velocities from sea-surface temperature, *J. Marine Res.* 64 (2006) 695–721.
- [16] J. Isern-Fontanet, G. Lapeyre, P. Klein, B. Chapron, M. W. Hecht, Three-dimensional reconstruction of oceanic mesoscale currents from surface information, *J. Geophys. Res.-Oceans* 113 (2008).
- [17] P. Klein, G. Lapeyre, G. Roullet, S. Le Gentil, H. Sasaki, Ocean turbulence at meso and submesoscales: connection between surface and interior dynamics, *Geophys. Astro. Fluid* 105 (2011) 421–437.
- [18] K. S. Smith, G. K. Vallis, The scales and equilibration of midocean eddies: Freely evolving flow, *J. Phys. Ocean.* 31 (2001) 554–571.
- [19] K. S. Smith, G. K. Vallis, The scales and equilibration of midocean eddies: Forced–dissipative flow, *J. Phys. Ocean.* 32 (2002) 1699–1720.
- [20] G. Roullet, J. McWilliams, X. Capet, M. Molemaker, Properties of steady geostrophic turbulence with isopycnal outcropping, *J. Phys. Ocean.* 42 (2012) 18–38.
- [21] A. Venaille, G. K. Vallis, K. S. Smith, Baroclinic turbulence in the ocean: Analysis with primitive equation and quasigeostrophic simulations, *J. Phys. Ocean.* 41 (2011) 1605–1623.
- [22] I. Shevchenko, P. Berloff, Multi-layer quasi-geostrophic ocean dynamics in eddy-resolving regimes, *Ocean Model.* 94 (2015) 1–14.
- [23] I. Grooms, L.-P. Nadeau, The effects of mesoscale ocean–atmosphere coupling on the quasigeostrophic double gyre, *Fluids* 1 (2016) 34.
- [24] G. R. Flierl, Models of vertical structure and the calibration of two-layer models, *Dyn. Atmos. Oceans* 2 (1978) 341–381.
- [25] B. A. Storer, F. J. Poulin, C. Ménesguen, The dynamics of quasigeostrophic lens-shaped vortices, *J. Phys. Ocean.* 48 (2018) 937–957.
- [26] K. S. Smith, J. Vanneste, A surface-aware projection basis for quasigeostrophic flow, *J. Phys. Ocean.* 43 (2013) 548–562.
- [27] F. Bretherton, Critical layer instability in baroclinic flows, *Q. J. Roy. Meteor. Soc.* 92 (1966) 325–334.
- [28] M. Watwood, I. Grooms, QG-Galerkin, <https://github.com/mwatwood-cu/QG-Galerkin>, 2018.
- [29] R. Tulloch, J. Marshall, C. Hill, K. S. Smith, Scales, growth rates, and spectral fluxes of baroclinic instability in the ocean, *J. Phys. Ocean.* 41 (2011) 1057–1076.